Magnetically induced lattice distortions in actinide compounds*

G. H. Lander and M. H. Mueller
Materials Science Division, Argonne National Laboratory, Argonne, Illinois 60439
(Received 8 October 1973; revised manuscript received 7 March 1974)

The lattice parameters of a number of actinide compounds have been measured at low temperature by x-ray diffraction. The ferromagnets NpN and NpC exhibit rhombohedral distortions at T_C. The antiferromagnets NpP and NpAs exhibit tetragonal distortions, which are compatible with the magnetic symmetry. In NpP the lattice distorts when the magnetic structure becomes commensurate with the atomic lattice. In NpAs the tetragonal distortion occurs at T_N, at which temperature the magnetic structure is a commensurate 4+, 4− arrangement. However, the magnetic structure of NpAs transforms to the simple type-I (+ −) arrangement at 142°K, and the x-ray experiments indicate that the lattice becomes cubic again at this temperature. X-ray experiments on the antiferromagnetic compounds UAs, NpSb, NpS, UO_2, and NpO_2 have failed to detect any lattice distortions, $|(c-a)/a| \leq 3\times10^{-4}$, in the magnetically ordered state. By listing all compounds examined, the presence of cubic or lower symmetry below the ordering temperature may be correlated with exchange interactions in the magnetic structures.

I. INTRODUCTION

The magnetic properties of actinide metals and compounds have been investigated at Argonne National Laboratory by a variety of experimental techniques.[1] The magnetic properties of the uranium monopnictides and monochalcogenides have been extensively documented,[2] and we have recently completed a study of the neptunium monopnictides.[3] (All these uranium and neptunium compounds have the NaCl crystal structure in the paramagnetic state.) Despite the wealth of experimental data available, the microscopic origins of magnetism and the numerous transitions in the actinide compounds are still not understood. On the other hand, our understanding of the magnetic interactions in the isostructural lanthanide compounds is reasonably complete. Neutron spectroscopy has provided a direct method of measuring the crystal-field splittings in these compounds,[4] and the competing exchange interactions have been obtained by analyzing the magnetic susceptibility.[5] Lévy[6] has reported that a number of lanthanide monopnictides exhibit structural distortions at their magnetic-ordering temperatures. These distortions are a consequence of the potential minima introduced by the crystal field acting on the free-ion configuration.[7] Lattice distortions have also been reported in NdS, DyS, and ErS,[8] and it seems likely that such distortions occur in most, if not all, lanthanide compounds that order magnetically. We exclude Gd^{3+} and Eu^{2+} compounds from consideration because the S-state ion is only weakly coupled to the lattice.

In contrast, Marples[9] has reported that UN and UP, both of which are type-I antiferromagnets, remain cubic below T_N, but that US and USe, which are ferromagnetic, exhibit trigonal (rhombohedral) distortions below T_C. We report the measurements of the lattice parameters between 5 and 350 °K of the following compounds: UAs, NpN, NpP, NpAs, NpSb, NpS, NpC, UO_2, and NpO_2; the last two compounds have the CaF_2 structure.

II. EXPERIMENTAL

The present experiments have been performed on pressed pellets (particle size ~40 μm). The samples were those used in previous experiments (usually neutron diffraction) in this Laboratory. Details of the samples preparation and characteristics may be found in the specific references for each compound. For the x-ray experiments, the powder was die pressed (527 kg/cm^2) into a flat disk and placed in a milled recess in a copper sample holder. The disk was covered with a Mylar window (0.005 cm thick) and sealed with a small copper frame and epoxy resin. Vacuum grease was used to attach the sample holder to a large copper block in a variable-temperature cryostat. Heaters and calibrated platinum and germanium resistors were embedded in the block. Temperature control to ±0.2 °K was attained with an exchange-gas system. Measurements were made on a conventional diffractometer table with filtered Cu $K\alpha$ radiation.

In the experiment, the diffraction profiles of the Bragg reflections were measured as a function of temperature. The major experimental problem was to obtain sufficient resolution so that the line broadening associated with a small lattice distortion could be observed. The experimental resolution is a function of both the instrument and the quality of the sample in terms of the absence of

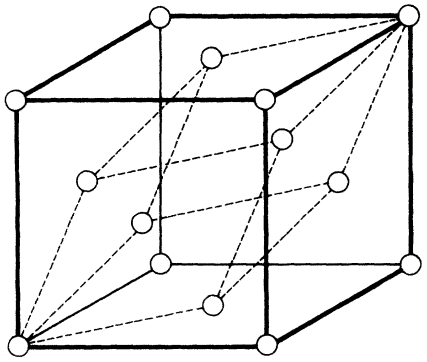

FIG. 1. Rhombohedral unit cell (dashed lines) with $\alpha = 60°$ drawn inside the face-centered-cubic cell.

strain and the presence of large domains. The instrumental resolution was determined experimentally by measuring the diffraction profile from an annealed tungsten specimen. The diffraction profile has a full width at half-maximum (FWHM) of 0.16° for $2\theta = 132°$. This FWHM is at least 50% smaller than that from even the best actinide sample, and, in these experiments, the limiting factor was the sample quality rather than the instrumental resolution. Fortunately, the diffraction profiles from most samples were sufficiently narrow (FWHM between 0.24° and 0.50°) that distortions of $\sim 5\times 10^{-4}$ could be detected. However, for NpSb, the diffraction profiles were quite broad, and additional annealing treatment did not significantly improve the linewidths. Another difficulty arises when moderately large single-crystal grains are present in the sample. Intense single-crystal-like "spikes" will then be superimposed on the smooth variation of intensity expected from a powder sample. Such effects were observed in the NpC sample, and made the determination of the extent of the lattice distortion difficult.

For trigonal distortions, the [111] axis of the cubic unit cell is chosen as the trigonal axis. When the distortion occurs, the [111] axis is either compressed or stretched. The new unit cell may be described as hexagonal or rhombohedral. For indexing on a hexagonal cell,

$$\vec{a}_H = 0.5(\vec{a}_c - \vec{c}_c) ,$$

$$\vec{b}_H = 0.5(\vec{b}_c - \vec{a}_c) ,$$

and

$$\vec{c}_H = (\vec{a}_c + \vec{b}_c + \vec{c}_c) ,$$

where the subscripts H and c refer to the hexagonal and cubic unit cells, respectively. If the unit cell is truly cubic, $c_H/a_H = \sqrt{6}$. The rhombohedral unit cell is shown in Fig. 1 and is possibly simpler to visualize than the hexagonal modification. The rhombohedral cell edge $a_R = a_c/\sqrt{2}$, and the rhombohedral angle α is 60° when the unit cell has cubic symmetry. An alternative description of the rhombohedral distortion is to define a length c as a distance along the unique trigonal axis and a as a distance in the plane perpendicular to c such that $c/a = 1.00$ in the cubic phase. This definition is especially useful when comparing the magnitude of trigonal and tetragonal distortions. In a tetragonal unit cell, the meanings of c and a follow crystallographic notation. The relationship between the change in the rhombohedral angle $\Delta\alpha$ from its (cubic) value of 60° and the c/a ratio is given by $\Delta\alpha = -4/\sqrt{27}\,(c-a)/a$ rad. Thus, if the [111] axis of the cube is compressed, $(c-a) < 0$, $\Delta\alpha > 0$, and hence $\alpha > 60°$, and the reverse is true if the [111] is stretched. (Marples[9] used a different rhombohedral cell, defining $\alpha = 90°$. The relationship between the 60° and 90° cells is such that $\Delta\alpha_{60°} = 2/\sqrt{3}\,\Delta\alpha_{90°}$. Levy[6] has used the 60° unit cell.)

In a cubic material, more than one Bragg reflection may often occur at the same scattering angle. For example, the (600) and (442) reflections occur at the same angle because $h^2+k^2+l^2 = 36$ for each set of planes. This reduces the sensitivity of experiments using powders because, to measure the distortions accurately, high-angle reflections need to be examined, and these are the reflections that are often multiple. In the present experiment, we have found only tetragonal and trigonal distortions. Initially, as these distortions develop, they result in a slight broadening of the x-ray lines. At this stage, an identification of the particular distortion may be difficult but is usually straightforward at the lowest temperatures (5 °K). The behavior of four cubic reflections in the presence of a small rhombohedral or tetragonal distortion is illustrated in Table I. (The rhombohedral distortion is

TABLE I. Reflections illustrating the relationship among the cubic, rhombohedral (indexed on the hexagonal cell), and tetragonal unit cells. The multiplicity of a set of equivalent planes $\{hkl\}$ is denoted as m.

	Cubic		Hexagonal		Tetragonal	
$h^2+k^2+l^2$	hkl	m	hkl	m	hkl	m
16	400	6	20.4	6	400	4
					004	2
36	600	6	30.6	12	600	4
	442	24	31.2	12	006	2
			10.10	6	442	8
					424	16
40	620	24	31.4	12	620	8
			21.8	12	602	8
					206	8
48	444	8	40.4	6	444	8
			00.12	2		

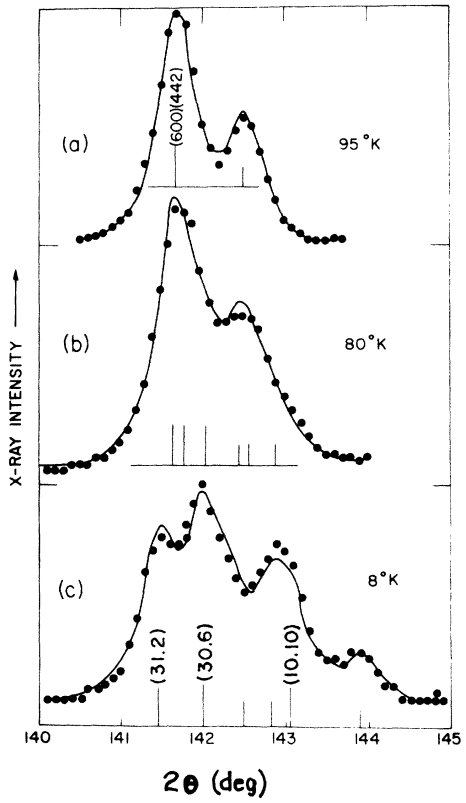

FIG. 2. X-ray intensity as a function of temperature for NpN. The continuous curves are least-squares fits to the experimental points. Below 87°K, NpN is ferromagnetic, and the cubic unit cell becomes rhombohedral. The indexing in the lower figure corresponds to a description on a hexagonal cell (see Sec. II). The vertical bars below each figure indicate the central positions of the α_1 and α_2 lines.

discussed here in terms of a hexagonal unit cell.) For example, the cubic (400) reflection splits if a tetragonal distortion occurs, but the cubic (444) reflection remains unsplit. For a rhombohedral distortion the opposite situation occurs. In the case of the $h^2+k^2+l^2=36$ and 40 reflections, the spectra will be complicated for both tetragonal and rhombohedral distortions. However, the sign of the distortion can be determined from the 36, but not from the 40, reflection because of the different multiplicities of the constituent reflections.

To obtain a quantitative measure of the lattice distortion, we have written a least-squares routine to fit a calculated x-ray profile to the experimental intensities. A simple Cauchy function has been found adequate in reproducing the observed profiles,[10]

$$y_{ij}=\frac{mL_pS}{\Delta}\Big/\left[1+\left(\frac{2\theta_j-2\theta_i}{\frac{1}{2}\Delta}\right)^2\right],$$

where y_{ij} is the intensity from a reflection $(hkl)_j$ at the position $2\theta_i$, m is the multiplicity of the reflection, L_p is the Lorentz-polarization factor, S is the scale factor, $2\theta_j$ is the calculated central position of the diffraction peak, and Δ is the FWHM of the diffraction profile. At the position $2\theta_i$, the total intensity is $\sum y_{ij}$, where the sum is over all reflections and all incident wavelengths (i.e., the α_1 and α_2 components). The parameters S, Δ, and the constant background level are obtained by measuring the diffraction profiles above the temperature of the distortion. As discussed above, the FWHM is basically a property of the sample homogeneity and strain and usually does not vary when the lattice distorts. The least-squares process rapidly converges and gives an excellent fit ($\chi^2\sim 1$) of the calculated and observed diffraction profiles. This analysis gives accurate values for the c/a ratio, which is the main interest in the experiment. To obtain absolute values of c and a, we have used a computer program that requires a series of diffraction peak positions as input.[11] In those samples in which no distortion was observed, the maximum possible value of $|(c-a)/a|$ was obtained as follows. First, the observed line profiles above the ordering temperature were reproduced accurately by the fitting process, then the calculated profiles that have increasing values of $(c-a)/a$ were compared with the diffraction data taken from the sample at low temperature. When the observed and calculated values of the FWHM differed by two standard deviations of the observed FWHM, the value of $(c-a)/a$ used in the calculation was taken as the maximum possible value.

III. RESULTS

A. NpN and NpC

Neptunium nitride and NpC are ferromagnetic and exhibit trigonal distortions. Neptunium nitride becomes ferromagnetic at $T_C=87$ °K.[3] In Fig. 2, we show the diffractometer outputs recorded from the NpN sample at three temperatures. In Fig. 2(a) the experimental points at 95 °K show the α_1, α_2 doublet of the (600)(442) Bragg reflection. The continuous curve is a least-squares fit to the experimental points and defines the instrumental constants and the unit-cell edge. At 80 °K, i.e., below T_C, Fig. 2(b) shows a broadening of the spectrum; note especially the change in the valley between the α_1 and α_2 peaks when comparing Figs. 2(a) and 2(b). In Fig. 2(c), the spectrum at 8 °K is clearly complex but is reproduced extremely well by the least-squares fitting process. The sharp single line (disregarding the α_2 component) above T_C is thus split into three lines in the ordered state, and are indexed on a hexagonal unit cell in Fig. 2(c). The least-squares procedure gives a

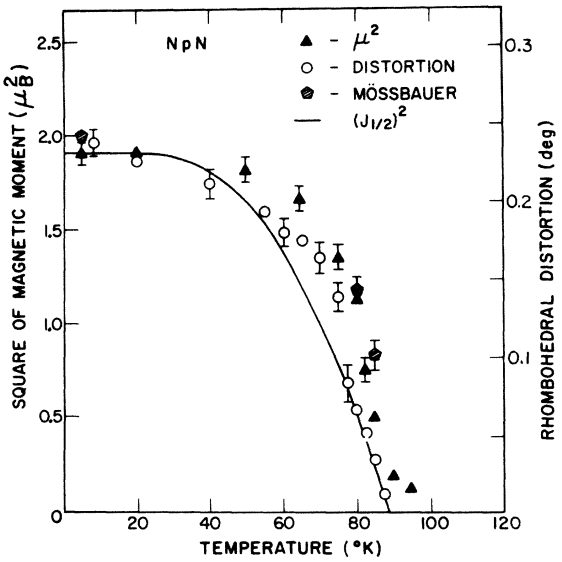

FIG. 3. Temperature dependence of the square of the magnetic moment (neutron diffraction), rhombohedral distortion (x rays), and the square of the hyperfine field (Mössbauer) in NpN. The solid curve is the $(J_{1/2})^2$ function.

precision of ± 3% when determining the magnitude of $|(c-a)/a|$ and, with this particular reflection (see Table I), the sign of $(c-a)$ is also uniquely determined by multiplicity considerations.

The temperature dependence of the rhombohedral distortion of the unit cell is shown in Fig. 3. Included in the figure is the temperature dependence of the square of the magnetic moment, as measured by neutron diffraction, and of the magnetic hyperfine field, as determined from the Mössbauer experiments. (See Ref. 3 for a more detailed discussion of these results.) Figure 3 demonstrates that in NpN the temperature dependence of the distortion does not scale with the square of the magnetic moment. If we consider the neutron results in Fig. 3 to represent $\langle M^2 \rangle$ as a function of temperature, then the lattice distortion approximately follows $\langle M^4 \rangle$. The lattice distortion in NpN is such that $\alpha > 60°$, the opposite sign of the distortion reported by Marples[9] in US and USe (see Table II).

Neptunium carbide orders antiferromagnetically at ~ 300 °K and has the type-I magnetic structure.[12] In this magnetic structure, ferromagnetic (001) planes are coupled antiferromagnetically in a simple alternating sequence. The direction of the magnetic moments is perpendicular to the ferromagnetic sheets and thus parallel to the c axis of this magnetic structure, which has tetragonal symmetry. At ~ 220 °K, NpC becomes ferromagnetic. Complications in NpC are that the compound exhibits a range of composition between $NpC_{0.82}$ and $NpC_{0.97}$, and the magnetic properties (particularly the Néel temperature) are partially dependent on the stoichiometry.[13] The room-temperature lattice parameter of the sample of NpC used in the x-ray experiments was 5.0051 ± 0.0003 Å. Such a value indicates a high-carbon content, and hence a Néel temperature of ~ 310 °K.[13] X-ray experiments with the sample between 220 and 350 °K indicate that the unit cell is cubic over this temperature range, and

TABLE II. Actinide compounds that have been examined at low temperature by x-ray diffraction. a_0 is the lattice parameter, α is the coefficient of thermal expansion between 200 °K and 300 °K, T_D is the temperature of the rhombohedral (R) or tetragonal (T) distortion. For a rhombohedral distortion, the change from the rhombohedral angle of 60° is given by $\Delta\alpha = -4/\sqrt{27}\ (c-a)/a$ rad, where the distances c and a are measured parallel and perpendicular to the trigonal axis, respectively. In the cubic phase, $c/a = 1.00$.

Material	Structure	a_0 (Å) at 300 °K	α (10^{-6}/°K)	T_C (°K)	T_N (°K)	Magnetic structure	T_D (°K)	Distortion	$10^4 \frac{c-a}{a}$ (± 3)
US	NaCl	5.489	9.8	178		F	178	R	+105
USe	NaCl	5.75	14.3	160		F	160	R	+ 81
NpC	NaCl	5.005	7.0	220		F	215	R	+23
NpN	NaCl	4.897	5.5	87		F	87	R	−52
NpP	NaCl	5.615	9.6		130	3+, 3−	74	T	−42
NpAs	NaCl	5.838	10.3		175	4+, 4−	175	T	−8
UN	NaCl	4.890	6.0		53	I			≤5
UP	NaCl	5.589	8.1		125	I			≤5
UAs	NaCl	5.779	9.2		127	I & IA			≤3
NpC	NaCl	5.005	7.0		310	I			≤5
NpAs	NaCl	5.838	10.3		(142)	I			≤3
NpSb	NaCl	6.254	17.0		207	I			≤15
NpS	NaCl	5.527	13.0		20	II			≤3
UO_2	CaF_2	5.470			31	I			≤3
NpO_2	CaF_2	5.434			24	?			≤3

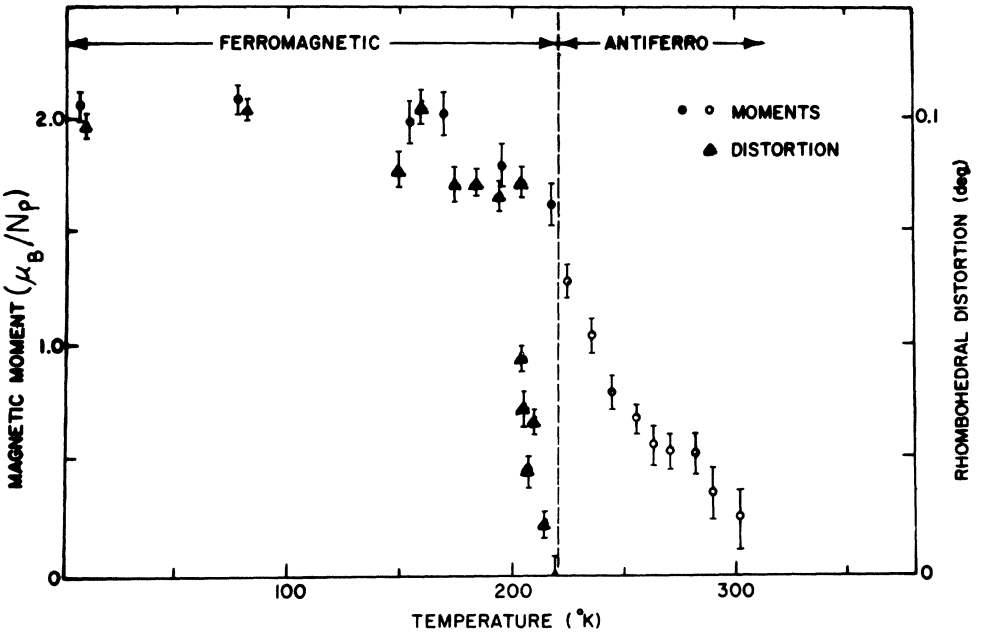

FIG. 4. Magnetic phase diagram, the ordered magnetic moment (both taken from Ref. 12), and the rhombohedral distortion in NpC as a function of temperature.

no distortion, $|(c-a)/a| \leq 5\times10^{-4}$, occurs in the type-I antiferromagnetic phase. In addition, no discontinuity was observed in the lattice parameter, and the thermal-expansion coefficient of $7\times10^{-6}/°K$ (see Table II) applies to both the para and antiferromagnetic phases. In Fig. 4, we show the temperature dependence of the rhombohedral distortion superimposed on the magnetic phase diagram given in Ref. 12. The over-all agreement between the calculated and observed diffraction profiles was worse in NpC than in the other compounds because of the large grains in the sample (Sec. II), but, despite these difficulties, the onset of the rhombohedral distortion appears to be almost first-order in nature and exhibits no appreciable hysteresis.

The rhombohedral distortion in NpC is clearly associated only with the ferromagnetic phase (see Fig. 4). However, the neutron data in Fig. 4, (taken from Ref. 12), were obtained from a sample of $NpC_{0.93}$. Although the ferromagnetic-antiferromagnetic transition temperature has been found to be almost independent of composition,[13] a direct determination of T_C in the present x-ray sample is desirable. To achieve this, we have performed a neutron experiment on the sample (1.1 g) used in the x-ray experiments. The neutron experiment involved the measurement of the depolarization of polarized neutrons transmitted through the sample as a function of temperature. Briefly, if a beam of neutrons polarized along the z axis ($P_z^i = 1.0$, $P_x^i = P_y^i = 0$) encounters a magnetic field with nonzero components H_x and H_y, the neutron will precess about these field components with a characteristic Larmor frequency. The final polarization vector will then have components other than in the z direction and, accordingly, the final value of $P_z^f < 1.0$. In the experiments, an analyzer crystal was placed behind the sample, and P_z^f was measured as a function of temperature. The depolarization is defined as $1-P_z$. To ensure $P_z^i = 1.0$ (actually 0.992 in the experiment) and magnetic saturation of the analyzer crystal, a 10-kOe field was applied to the sample and analyzer. The temperature was measured with a calibrated GaAs diode, which is accurate to ± 1 °K over the temperature range of interest. To determine P_z^f, the ratio R of spin-up to spin-down neutron intensity reflected from the (200) Bragg reflection of the analyzer crystal was measured. In the antiferromagnetic state, fluctuations of the magnetization are less than one atomic unit cell, whereas the Larmor precession distance for 1 – Å neutrons is ~ 100 μm. Under these conditions the depolarization is zero (apart from a very small depolarization caused by quantum adiabatic processes) and $P_z^f = P_z^i$ with $R \sim 150$. In a ferromagnetic material in which the magnetic domains and the Larmor precession distance are comparable in size, the domains with their magnetization direction at any angle to H_z will contribute to neutron depolarization. This is indeed the case, and $R = 1.5$ at 5 °K,

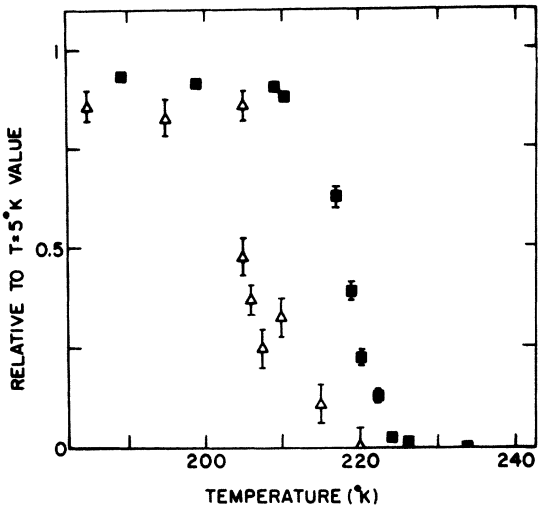

FIG. 5. Relative values of the depolarization of polarized neutrons transmitted through the sample ■, and the lattice distortion Δ, as a function of temperature for NpC.

corresponding to a depolarization of 0.8. In Fig. 5, the depolarization and lattice distortion relative to their values at 5 °K are plotted as a function of temperature in the region of the ferro to antiferromagnetic transition. Figure 5 demonstrates that T_C for this sample is between 220 and 223 °K, which is in excellent agreement with previous magnetization and neutron experiments, but that T_C is some 5 to 7 °K *above* the temperature at which the rhombohedral distortion occurs. We should emphasize that in all other actinide compounds examined to date, the distortion temperature T_D and the magnetic-ordering temperature coincide within experimental accuracy. Of course, the ferro to antiferro transition is unique to NpC, and the exceptional nature of T_D may not be too surprising.

B. NpP and NpAs

The magnetic structure[14] and the lattice distortion[15] in NpP have been the subjects of separate publications. Briefly, NpP becomes antiferromagnetic at $T_N = 130$ °K. The initial magnetic ordering is incommensurate with the chemical unit cell and is characterized, as in the type-I structure, by ferromagnetic (001) sheets with the spin direction perpendicular to the sheets, i.e., $\vec{\mu} \parallel [001]$. The magnetic symmetry is tetragonal. At 74 °K, the neutron-diffraction experiments[14] indicate that the magnetic structure becomes commensurate with the atomic lattice with a repeat distance of three chemical unit cells. The structure may be described approximately as a 3+, 3− arrangement of ferromagnetic (001) sheets. The results of the x-ray experiments are shown in Fig. 6. No anomaly in the lattice constant is observed at the Néel temperature, but at (74.5 ± 0.3) °K a large tetragonal distortion is observed. The c/a ratio (see insert of Fig. 6) changes abruptly to 0.9975 on cooling 5 °K below the transition and reaches a value of 0.9958 ± 0.0002 at helium temperature. The volume of the unit cell ($=a^2c$) shows a discontinuity at 74 °K and expands below this temperature. The volume discontinuity at the incommensurate-commensurate transition implies that the transition is first order.

Neptunium arsenide becomes antiferromagnetic at $T_N = 175$ °K. Neutron-diffraction experiments[3] indicate that the magnetic structure between ~ 145 and 175 °K is a 4+, 4− configuration that is commensurate with the chemical unit cell. Below ~ 150 °K, reflections from the type-I arrangement (i.e., a simple + − configuration) begin to appear in the neutron pattern, and the 4+, 4− arrangement is not stable below 140 °K. The type-I structure is present at all lower temperatures. The spin direction in NpAs is perpendicular to the ferromagnetic (001) sheets at all temperatures below T_N, so that, as in NpP, the magnetic symmetry is tetragonal. The behavior of the lattice parameters of NpAs is shown in Fig. 7. The material becomes tetragonal at (175 ± 2) °K, (i.e., at T_N. By 143 °K, the c/a ratio has attained a value of 0.9992 ± 0.0002 and is varying in approximately the same manner as that of NpP (see Fig. 6). On further cooling to 142 °K, a first-order transition occurs such that the material again *becomes cubic*. A discontinuity in the volume of the unit cell is observed; the volume at 143 °K is 198.20 ± 0.07 Å^3 and at 142 °K 198.65 ± 0.05 Å.^{3} Almost no hysteresis (≤ 0.5 °K) is associated with the 142 °K transition, which is surprising in view of the large polycrystalline sample used in the experiments and the rather sluggish transformation observed in the neutron experiments. Below 142 °K, the x-ray

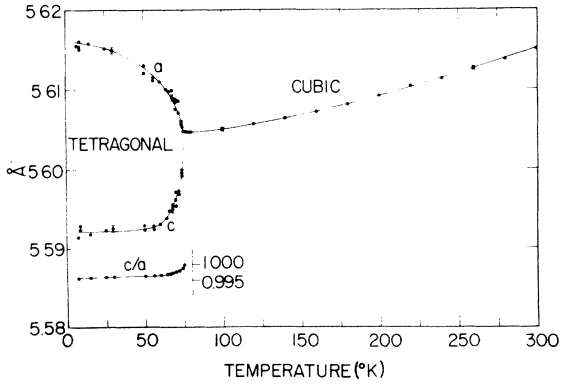

FIG. 6. Variation of the lattice parameter of NpP with temperature. The variation of the c/a ratio in the tetragonal region is also shown.

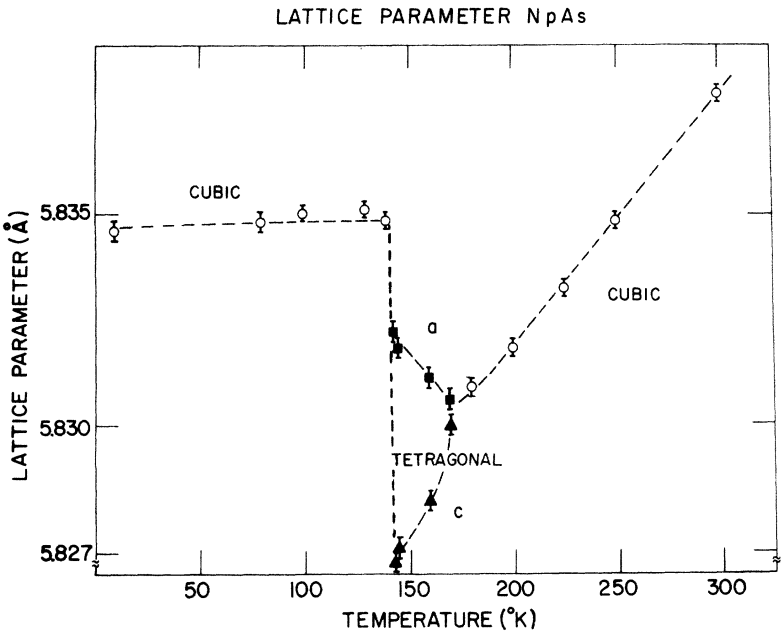

FIG. 7. Variation of the lattice parameters of NpAs with temperature.

diffraction peaks are slightly broader than in the high-temperature cubic and tetragonal phases. For example, the (444) reflection ($2\theta = 132°$) has a FWHM of $0.23 \pm 0.01°$ in the high-temperature cubic and tetragonal phases [the (444) reflection is not split by the tetragonal distortion] but has a FWHM of $0.27° \pm 0.01°$ at 140 °K. This width gradually decreases as the temperature is lowered, and the value at helium temperature is again 0.23°. No simple explanation can be advanced for this line broadening. The abrupt transition may result in strain in the powder sample, although it seems unlikely that this strain would be annealed out at lower temperatures. Alternatively, the broadening may be a result of dynamic effects, such as magnetic exciton-phonon coupling, following the transition. The absence of any tetragonal distortion at 5 °K may be characterized by the quantity $|(c-a)/a| \leq 3 \times 10^{-4}$.

C. UAs, NpSb, NpS, UO_2, and NpO_2

These five compounds are antiferromagnetic, but no crystallographic distortions have been observed below their respective ordering temperatures. They thus fall into the same category as UN and UP.[9] Uranium arsenide[16] becomes antiferromagnetic at 127 °K with a type-I magnetic structure. At 63 °K, a second transition, which also involves an increase in the value of the ordered moment, occurs and the magnetic structure below 63 °K is the type-IA [2+, 2− arrangement of ferromagnetic (001) sheets]. The x-ray experiments indicate no discontinuity in the cubic lattice parameter at 127 °K but do indicate a small expansion of the unit cell below 63 °K. The behavior of the lattice parameter of UAs resembles that of UP (see Fig. 1 of Ref. 9), in which a small expansion is observed below the "moment-jump" transition at 22 °K in UP. As indicated in Table II, any lattice distortion in UAs is less than 3×10^{-4}. The lower limit of any possible distortion in UN or UP was not given by Marples,[9] but, in view of the similar experimental method, we have assigned a value of 5×10^{-4} in Table II.

Neptunium antimonide becomes antiferromagnetic at $T_N = 207$ °K with the type-I magnetic structure.[3] As discussed in Sec. II, the x-ray diffraction profiles were quite broad in NpSb, and a rather high limit for the lack of a distortion is given in Table II.

Neptunium sulfide becomes antiferromagnetic at $T_N = 20$ °K with the type-II magnetic structure in which ferromagnetic (111) sheets are coupled antiferromagnetically.[17] Within a ferromagnetic sheet, the magnetic moments are parallel to a cube edge. The x-ray experiments indicated a small discontinuity in the lattice parameter at 20 °K, but no lattice distortion was observed.

The magnetic properties of UO_2 (CaF_2 crystal structure) have been examined thoroughly. The compound orders magnetically at 31 °K with a first-order transition to the type-I antiferromagnetic structure.[18] The magnetic moments in UO_2 lie in the (001) ferromagnetic sheets, rather than perpendicular to them as in the other type-I magnetic structures discussed in the present paper. Pirie and Smith[19] were unable to detect any static atomic displacement in UO_2 below T_N, but they did

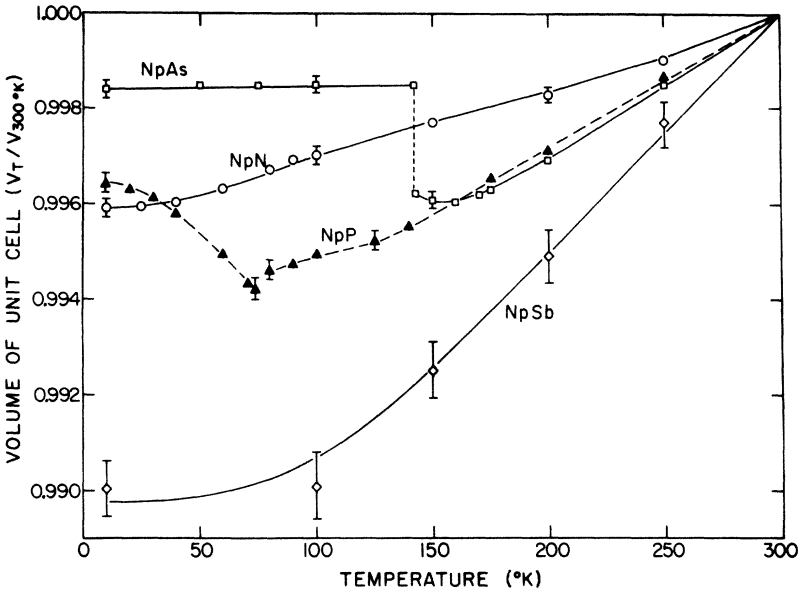

FIG. 8. Temperature dependence of the unit-cell volume (relative to the value at 300°K) for the neptunium monopnictides.

not search for any possible lattice distortion. Brandt and Walker[20] have made strain-gauge measurements on single crystals and observed a fractional length discontinuity of 5×10^{-5} at T_N in the ⟨100⟩ direction. Since the c axis of the magnetic structure in UO_2 can be any one of the three cube axes in the single crystal, bulk measurements, such as the strain-gauge technique, cannot provide information about a lattice distortion unless a single magnetic domain can be produced. (Strictly speaking, the magnetic symmetry of UO_2 is lower than tetragonal. We might, therefore, expect an initial tetragonal distortion followed by a smaller orthorhombic or monoclinic distortion, such as is observed in DySb.[21]) The length discontinuity of 5×10^{-5} is below our sensitivity of $\sim10\times10^{-5}$ with polycrystalline samples. No lattice distortion was observed in UO_2.

Measurements of the magnetic susceptibility[22] of NpO_2 suggest a magnetic transition at ~ 25 °K, but neutron experiments[23] failed to observe any magnetic reflections in the neutron-diffraction pattern at low temperatures. A subsequent Mössbauer study[24] showed that the ordered magnetic moment, if present, was of the order of $0.01\mu_B$/neptunium atom. Our x-ray experiments have found no evidence for a lattice distortion or a discontinuity in the lattice parameter below 25 °K.

IV. DISCUSSION

The magnetic transitions that occur in many of these compounds are closely coupled to the behavior of the lattice, as observed by x-ray diffraction. The volume change relative to the room-temperature value for the neptunium monopnictides is shown in Fig. 8 as a function of temperature. At high temperatures, the straight-line behavior reflects the regular thermal expansion of the lattice and, as expected, the thermal expansion is greater for the compounds with greater interatomic spacings. The coefficients of thermal expansion for the uranium and neptunium compounds are comparable in magnitude. The volume contractions in NpN (T_C = 87 °K) and NpSb (T_N = 207 °K) vary smoothly through the transitions, indicating that they are not first order. Similarly, second-order transitions occur at T_N in NpP (130 °K) and NpAs (175 °K). However, at lower temperatures NpP and NpAs exhibit first-order transitions, in which a discontinuity occurs in the volume of the unit cell. The distortion from tetragonal to cubic within the ordered state in NpAs (Fig. 7) is, as far as we know, unique.

The results of the present experiments are conveniently summarized in Table II, which also includes the results from Ref. 9. (A rhombohedral distortion, but not its magnitude, has been reported in ferromagnetic UTe.[2]) One of the most striking features of Table II is the number of actinide materials that apparently remain cubic in the ordered regime. The presence of cubic symmetry below T_N is not confined to type-I antiferromagnets with $\vec{\mu}\parallel[001]$, e.g., UN, UP, UAs (T > 63 °K), NpAs (T < 142 °K), NpC (T > 220 °K), and NpSb, but is also observed in the type-IA arrangement in UAs (T < 63 °K), in the type-I structure with moments in the (001) plane as found in UO_2, and in the Type-II arrangement as in NpS. In absolute terms we cannot, of course, say that *no* distortion occurs in the compounds listed in the

lower part of Table II. The lower limit of 3×10^{-4} is still considerably above the distortions that can be detected by using single crystals with either strain-gauge[25] or x-ray techniques.[26] Unfortunately, apart from UO_2, suitable single crystals are presently unavailable. The lattice distortions reported by Lévy[6] on single crystals of the lanthanide monopnictides range from 10 and 70 ($\times10^{-4}$). Even if small lattice distortions are subsequently found in some of the compounds listed in the lower half of Table II, it is clear that a major difference exists between the entries in the upper and lower halves of Table II.

A correlation in Table II is that all actinide ferromagnets examined to date exhibit rhombohedral distortions. From symmetry considerations, the rhombohedral distortion in these ferromagnets indicates that the easy axis of magnetization is in, or perpendicular to, the (111) plane. This hypothesis has been confirmed directly in US, in which magnetization[27] and neutron[28] experiments on single crystals have determined that the magnetic moments are parallel to the unique trigonal axis. Neutron-diffraction experiments on polycrystalline ferromagnets (for example, those on NpN and NpC) cannot determine the spin direction, and the inference drawn from the x-ray experiments about this direction provides important new information about these systems. The situation in NpC is particularly unusual. In the antiferromagnetic state [(220–310) °K], the spin direction is along the cube edge, but a spin rotation must occur at ~ 220 °K because a trigonal distortion is observed in the ferromagnetic state (T < 220 °K).

The lattice behavior listed in Table II cannot be understood in terms of the crystal-field interactions that play a dominant role in the isostructural lanthanide compounds. As described by Stevens and Pytte,[7] trigonal distortions are expected for $5f^1$, $5f^4$, and $5f^5$ configurations, and tetragonal distortions are expected for $5f^2$ and $5f^3$ depending on the sign of $\langle J \| \beta \| J \rangle$. Irrespective of the electron configurations assumed for the compounds in Table II,[1–3] the crystal-field scheme cannot be used to understand the behavior of the lattice parameters. Alternatively, we seek a correlation that involves the exchange interactions in the magnetic structures. Such a scheme is suggested by examining Table II. First, we note that all magnetic structures may be described in terms of ferromagnetic sheets stacked in a certain sequence. Summing over the magnetic unit cell, the interactions *between* these ferromagnetic sheets may be all antiferromagnetic (types-I and -II structures), all ferromagnetic (US, NpN, etc.), or a mixture ($n+$, $n-$ structures where $n>2$). *In those materials in which the ferromagnetic outnumber the antiferromagnetic interactions, a crystallographic distortion is observed.* Thus all ferromagnets distort at T_C. For the antiferromagnets of the form $n+$, $n-$, the type-IA structure ($n=2$) has two ferro and two antiferromagnetic interactions, but for $n>2$ the ferromagnetic interactions dominate. For example, in NpP where $n=3$, four ferro and two antiferromagnetic interactions between the sheets are present in one magnetic unit cell. We anticipate, of course, that exceptions to this "rule" will be found, although it is remarkable that so many compounds fit with such a simple scheme. Notice, in particular, that NpAs and NpC appear twice in Table II. In both materials, the lattice is cubic when the antiferromagnetic structure is type-I but distorts to tetragonal in NpAs and rhombohedral in NpC—both distortions are consistent with the simple scheme outlined above.

Although we are unable to offer any definitive explanation for this correlation, the magnon-phonon coupling demonstrated in UO_2,[29] provides one possible mechanism for stabilizing the lattice against crystallographic distortions. Further experiments, such as the measurement of the elastic constants and inelastic-neutron scattering, will be of considerable interest when single crystals of these compounds become available.

ACKNOWLEDGMENTS

It is a pleasure to thank H. W. Knott for valuable experimental assistance and J. F. Reddy for his care and ingenuity in sample preparation and encapsulation.

---

*Work performed under the auspices of the U. S. Atomic Energy Commission.

[1]For a recent review see M. B. Brodsky, AIP Conf. Proc. 5, 611 (1972).

[2]J. Grunzweig-Genossar, M. Kuznietz, and F. Friedman, Phys. Rev. 173, 562 (1968); M. Kuznietz, in *Rare Earths and Actinides* (Institute of Physics, London, 1971), p. 162; F. A. Wedgwood and M. Kuznietz, J. Phys. C 5, 3012 (1972).

[3]A. T. Aldred, B. D. Dunlap, A. R. Harvey, D. J. Lam, G. H. Lander, and M. H. Mueller, Phys. Rev. B 9, 3766 (1974).

[4]K. C. Turberfield, L. Passell, R. J. Birgeneau, and E. Bucher, Phys. Rev. Lett. 25, 752 (1970) J. Appl. Phys. 42, 1746 (1971); A. Furrer, J. Kjems, and O. Vogt, J. Phys. C 5, 2246 (1972).

[5]B. R. Cooper and O. Vogt, Phys. Rev. B 1, 1218 (1970); Y. L. Wang and B. R. Cooper, *ibid.* B 2, 2607 (1970).

[6]F. Lévy, Phys. Kondens Mater. 10, 85 (1969).

[7]K. W. H. Stevens and E. Pytte, Solid State Commun. 13, 101 (1973).

[8]L. J. Tao, J. B. Torrance, and F. Holtzberg, 19th

Conference on Magnetism and Magnetic Materials, Boston, Nov. 1973, Abstract 1D-4 (unpublished).
[9]J. A. C. Marples, J. Phys. Chem. Solids 31, 2431 (1970).
[10]E. R. Pike, Acta Crystallogr. 12, 87 (1959).
[11]M. H. Mueller, L. Heaton, and K. T. Miller, Acta Crystallogr. 13, 828 (1960).
[12]G. H. Lander, L. Heaton, M. H. Mueller, and K. D. Anderson, J. Phys. Chem. Solids 30, 733 (1969).
[13]D. J. Lam, M. H. Mueller, A. P. Paulikas, and G. H. Lander, J. Phys. (Paris) 32, C1-917 (1971).
[14]G. H. Lander, B. D. Dunlap, M. H. Mueller, I. Nowik, and J. F. Reddy, Int. J. Magnetism 4, 99 (1973).
[15]M. H. Mueller, G. H. Lander, H. W. Knott, and J. F. Reddy, Phys. Lett. 44A, 249 (1973).
[16]J. Leciejewicz, A. Murasik, and R. Troc, Phys. Status Solidi 30, 157 (1968); 38, K89 (1970); G. H. Lander, M. H. Mueller, and J. F. Reddy, Phys. Rev. B 6, 1880 (1972).
[17]D. J. Lam, B. D. Dunlap, A. R. Harvey, M. H. Mueller, A. T. Aldred, I. Nowik, and G. H. Lander, International Conference on Magnetism, August 1973, Moscow, Abstract 28mS7 (unpublished), and to be published.
[18]B. C. Frazer, G. Shirane, D. E. Cox, and C. E. Olsen, Phys. Rev. 140, A1448 (1965).
[19]J. D. Pirie and T. Smith, Phys. Status Solidi 41, 221 (1970); and private communication.
[20]O. G. Brandt and C. T. Walker, Phys. Rev. 170, 528 (1968); Phys. Rev. Lett. 18, 11 (1967).
[21]G. P. Felcher, T. O. Brun, R. J. Gambino, and M. Kuznietz, Phys. Rev. B 8, 260 (1973).
[22]J. W. Ross and D. J. Lam, J. Appl. Phys. 38, 1451 (1967).
[23]D. E. Cox and B. C. Frazer, J. Phys. Chem. Solids 28, 1649 (1967); L. Heaton, M. H. Mueller, and J. M. Williams, *ibid.* 28, 1651 (1967).
[24]B. D. Dunlap, M. B. Brodsky, G. M. Kalvius, G. K. Shenoy, and D. J. Lam, J. Appl. Phys. 40, 1495 (1969).
[25]In chromium, for example, strain-gauge measurements have shown the presence of a distortion of 5×10^{-6}; see M. O. Steinitz, L. H. Schwarz, J. A. Marcus, E. Fawcett, and W. A. Reed, Phys. Rev. Lett. 23, 979 (1969).
[26]Again in chromium, F. H. Combley [Acta Crystallogr. B 24, 142 (1968)] gave a lower limit of 1×10^{-5} using x-ray techniques.
[27]W. E. Gardner and T. F. Smith, Proceedings of the International Conference on Low Temperature Physics (University St. Andrews, Printing Office, Scotland, 1968), Vol. 2, p. 1377.
[28]F. A. Wedgwood, J. Phys. C 5, 2427 (1972).
[29]R. A. Cowley and G. Dolling, Phys. Rev. 167, 464 (1968); S. J. Allen, *ibid.* 166, 530 (1968); 167, 492 (1968).